

Ontogeny and adaptivity in a model protocell

Eran Agmon^{1,2}, Alexander J. Gates^{2,1} and Randall D. Beer^{1,2}

¹ Cognitive Science Program, Indiana University, Bloomington, IN 47406, USA

² School of Informatics and Computing, Indiana University, Bloomington, IN 47406, USA
agmon.eran@gmail.com

Abstract

Viability, ontogeny, and adaptivity have been widely discussed within the context of emergent individuality. This paper provides an initial step towards a more formal treatment of these concepts. A network of possible ontogenies is uncovered by subjecting a model protocell to sequential perturbations, and mapping the resulting structural configurations. The analysis of this network reveals trends in how the protocell can move between configurations, how its morphology changes, and how the role of the environment varies throughout. Viability is defined as expected lifespan given an initial configuration. This leads to two notions of adaptivity: a local adaptivity that addresses how viability changes in plastic transitions, and a global adaptivity that looks at longer-term tendencies for increased viability. The mechanisms of a minimal adaptive transition are analyzed, and it is shown that these rely on distributed spatial processes rather than an explicit regulatory mechanism.

Introduction

Biological individuals are a special class of physical systems that counter the universal trend towards disintegration. In any given moment, a physical system can be described by its structural configuration — the spatial arrangement of components from which it is constituted. The states and locations of these components unfold dynamically, and whereas most configurations tend towards a uniform equilibrium, biological individuals are a unique subclass of physical system that persist as individuals. The theory of autopoiesis argues this viability comes from their closure of production; as a result of their intrinsic dynamics and material exchange with the environment, biological individuals produce and distribute the materials needed to stabilize themselves [10].

From the perspective of an individual, an environment appears as a probability distribution over possible perturbations. These perturbations, together with the individual's intrinsic dynamics, determine the individual's subsequent states. Thus, a perturbation can have one of three consequences: the individual can be unaffected (a robust transition), it can be changed to a different viable configuration (a plastic transition), or it can cross into the set of nonviable configurations and disintegrate (a destructive transition).

An individual that remains viable for any length of time experiences a sequence of perturbations that induce a corresponding sequence of configurational changes. In this paper, we refer to an unbroken trajectory through the set of viable configurations as an *ontogeny*; when the trajectory crosses the boundary of viability into a nonviable region, closure of production is broken and the ontogeny ends. Different sequences of perturbations have the potential to induce different ontogenies. If the set of possible perturbations is known, one can in principle map the entire network of possible transitions that an individual can undergo.

The *viability* of any configuration in an ontogenic network can be defined as the average number of perturbations it is from disintegration, weighted by the probability of those perturbations. If many perturbations are needed to destroy a configuration, then it is highly viable; if few are needed, then it has lower viability. *Adaptivity* can be defined as the change in viability that follows plastic transitions. Taken locally, *adaptive transitions* are plastic transitions in which viability is increased, and *maladaptive transitions* are those in which viability is reduced. A more global notion of adaptivity addresses whether there are trends towards increased viability across possible ontogenies. This could be achieved in a variety of ways, ranging from an explicit regulatory subsystem [3; 6] to more emergent processes.

In this paper, the relationship between viability, ontogeny, and adaptivity is investigated in the context of a model protocell that we recently proposed [1]. After reviewing the model and describing the environment in which we place it, the paper is organized as follows. First, we build upon a framework for exploring ontogenies as a network structure [4]. Applying this methodology reveals a rich complexity of ontogenic structure, which we characterize through a combination of graph-theoretic, morphology-based, and statistical measures. Second, viability is measured for all configurations across the ontogenic network, and increases in the measure allow us to identify trends of adaptive change. Finally, the mechanisms of an adaptive transition are analyzed in great detail.

A model of emergent individuality

An essential feature of biological individuals is their emergence from material components. To develop a theoretical understanding of such systems, the models must also display an emergence of individuality in the sense that they should exhibit metabolism-boundary co-construction. While such emergence has been explored in systems with abstract physics, such as the Game of Life [4], the model described here moves towards a more realistic chemistry.

The spatial model of molecular concentration dynamics considered here includes the diffusion, repulsion, chemical reactions, and decay of four molecular species: membrane (M), autocatalyst (A), food (F), and water (W). The chemical reactions are such that A is produced from an autocatalytic reaction between A and F , while M molecules are produced by a reaction which consumes both A and F . Both A and M also decay at a constant rate. Considered individually, molecular concentrations diffuse across a 2-dimensional lattice at a constant rate. However, the presence of repulsion between molecular types breaks the traditional symmetries. Based on the behavior of phospholipid bilayers, the model implements anisotropic repulsion between membrane molecules M and both A and W . This requires the introduction of a fifth state variable, θ , which defines the orientation of M and behaves with its own dynamic of alignment with neighboring orientations. Here, we utilize a 40×40 lattice. Each lattice point has the five state variables, resulting in an 8000-dimensional coupled dynamical system. For specific details of the model's implementation, refer to [2].

The model displays two distinct types of equilibrium points: the uniform equilibrium point with zero concentrations of both A and M , and stable inhomogeneities in which positive concentrations of A and M are maintained. The system is considered stable when the average temporal derivatives of A and M over the entire lattice satisfies $\frac{1}{2} \sum_{m \in \{A, M\}} \sum_{x_{ij}} |\dot{m}(x_{ij}, t_k)| < \epsilon_1$ for all $t_k \in [t, t + 1000]$ for a sufficiently small $\epsilon_1 = 0.05$. Even though these configurations are equilibrium points, they are still chemically active, with positive diffusion and reaction rates. It was demonstrated that, in the later class of equilibrium points, M was necessary to contain A at concentrations high enough such that A could continuously construct both A and M faster than their molecular decay. Thus, these configurations exhibit metabolism-boundary co-construction [2].

Throughout this work, we study the ontogeny of a particular configuration we named SC (stable configuration), shown on the left side of Figure 1. Due to θ 's initialization, SC has broken symmetries across both its horizontal and vertical axes.

Environment as perturbation

From the individual's point of view, an environment is a probability distribution over a set of perturbations. We consider an environment \mathcal{E} , which consists of perturbations that

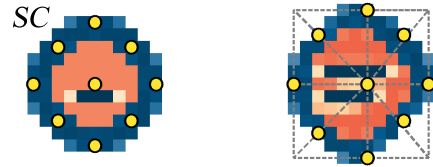


Figure 1: SC is the configuration on the left, which provides the starting point for this paper's exploration of ontogenic networks. These diagrams show only the autocatalyst (red) and membrane (blue) concentrations; food and water have been removed for clarity. The 9 relative perturbation locations from \mathcal{E} are denoted by yellow dots. The right figure shows how locations are determined: a box encapsulates the configuration, and focal points are centered on the lattice cells according to intersections with the box's lines.

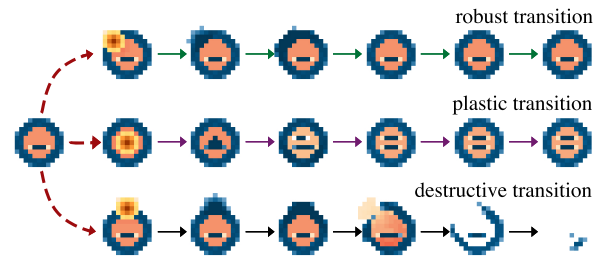


Figure 2: Three perturbations from environment \mathcal{E} applied to SC . The perturbations increase the membrane concentration with the same amplitude $\alpha = 2$, as shown in yellow. Following perturbation, the system undergoes transients that stabilize in different attractor classes. The top branch shows a robust transition that returns to the original configuration, the middle branch shows a plastic transition that brings the system to a different stable configuration, and the bottom branch shows a destructive transition.

increase the concentration of either autocatalyst (A) or membrane (M) in the local neighborhoods of nine distinct focal points. These locations are specified relative to the given configuration according to an algorithm that guarantees placement on the configuration (Figure 1). The increase in concentration is determined by a Gaussian function of the form: $G(x_{ij}) = \alpha e^{-(|x_{ij} - x_f|)^2 / 2\sigma^2}$, where $|x_{ij} - x_f|$ is the distance from the focal point x_f to the given cell x_{ij} , α is the magnitude of the function, and $\sigma^2 = 2.0$ determines its width. Four different magnitudes of $\alpha = [0.5, 1, 1.5, 2]$ are used. In total, environment \mathcal{E} consists of 72 possible perturbations, each of which occurs with a uniform probability.

Once a perturbation is applied, it instantaneously displaces the system in state space. The system dynamics then unfold towards a limit set, resulting in one of three classes of possible outcomes: the uniform state, the same viable con-

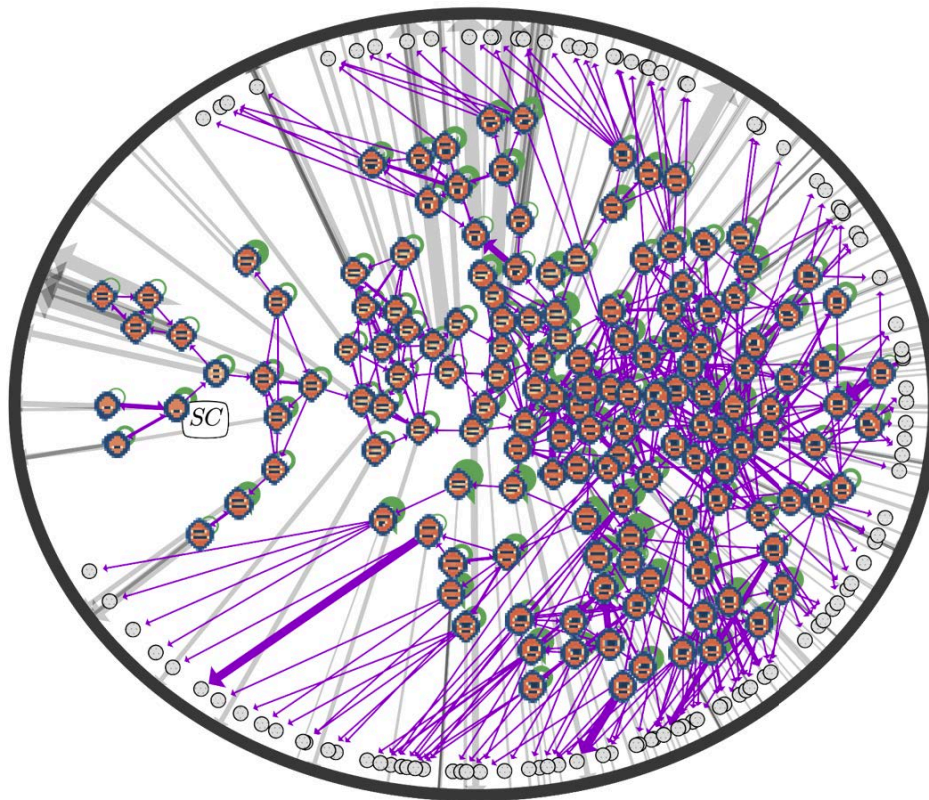


Figure 3: The ontogenic network ON captures the structure of all possible ontogenies starting at SC in environment \mathcal{E} . All configurations' morphologies are shown as nodes while the death state is depicted as a black ellipse. Unsearched configurations are denoted as gray nodes. Directed edges capture the transitions between configurations and are categorized as robust (green self-loops), plastic (purple edges), and destructive (gray edges). Edge width represents the log-probability for each transition.

figuration, or a different viable configuration. Examples of these three possibilities are illustrated in Figure 2.

To determine the identity of the resulting configuration, C , a comparison metric is used within the 3200-dimensional state space of M and A molecular concentrations (40x40 lattice sites for two molecule types). The structural distance from each previously observed configuration, C' , is found by taking the summed absolute difference between the configurations' states $d(C, C') = \sum_{m \in \{A, M\}} \sum_{x_{ij}} |m_C(t, x_{ij}) - m_{C'}(t, x_{ij})|$. If this sum satisfies $d(C, C') < \epsilon_2$ with $\epsilon_2 = 1.0$, then we consider the configurations equivalent.

Ontogenic networks

Typical environments are the source of repeated perturbations which induce a sequence of changes to an individual's structure. A single trajectory through the set of viable configurations is an ontogeny. Different perturbations have the potential to induce different plastic transitions, resulting in different ontogenic trajectories. The structure of all possible ontogenies defines an *ontogenic network*, in which the viable configurations and death state constitute the net-

work's nodes, and each environmental perturbation is a directed edge. Given a specific individual's configuration in a specific environment, the full ontogenic network is obtained by exhaustively characterizing the configuration's response to every environmental perturbation. The process is then repeated for all subsequent configurations until closure is achieved (i.e. every transition results in either a previously characterized configuration or death) [4].

The full ontogenic network formed by SC 's repeated exposure to environment \mathcal{E} is a multigraph with a set of reachable configurations as its nodes, each of which is the source for 72 directed edges. Following each perturbation, the system was given sufficient time to relax back to a stable condition before the next perturbation was applied. The network was generated by a breadth-first search that exposed all configurations to \mathcal{E} as they were discovered. For this paper, the search was terminated at a uniform depth of 16 from SC . Configurations on the unsearched frontier are excluded from this section's analysis.

As a first step towards characterizing the structure of this network, we focus on the relationships between viable configurations. This suggests reducing the full ontogenic net-

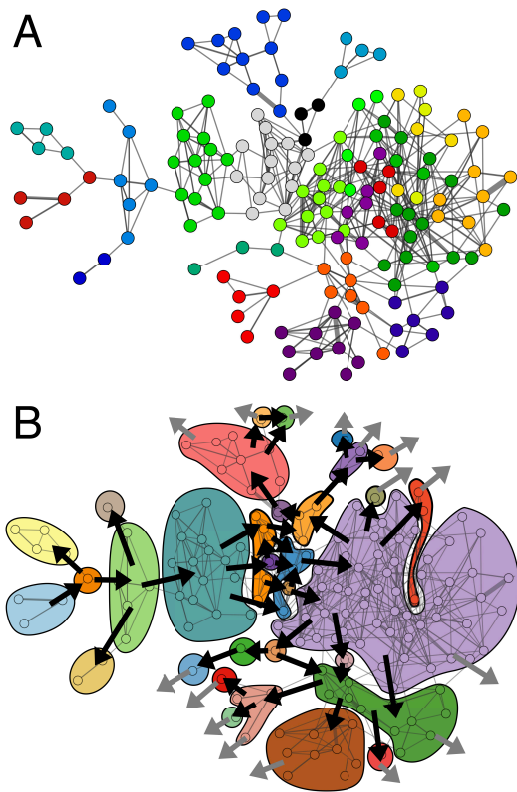


Figure 4: Two copies of *ON* (with the same layout as Figure 3). A) *ON*'s nodes are colored by cluster membership in InfoMap communities. B) Strongly connected components are shown as colored regions, with arrows indicating the direction of ontogenic change. Gray arrows indicate transitions to the unsearched frontier.

work by combining edges according to equivalence classes of transition outcome and considering the death state with all destructive transitions separately from the rest of the network. The resulting reduced ontogenic network (*ON*) is shown in Figure 3. *SC*'s initial asymmetry is propagated through all configurations in *ON*. In theory, mirrored initial conditions can yield ontogenies identical to *ON*, but with mirrored configurations.

Remarkably, this pairing of a simple configuration and environment generates an extensive ontogenic network, rich with features. It has 154 stable configurations (represented in the figure by the morphological structure of *A* and *M* concentrations) as nodes while the death state is shown by the surrounding black ellipse. The directed edges in *ON* reflect the probability for a transition to occur given a random perturbation from the environment, with robust transitions shown as green self-loops, plastic transitions shown as directed purple edges between configurations, and destructive transitions shown in gray.

A statistical analysis of *ON* reveals that configurations vary widely in their response to perturbations from \mathcal{E} . Ro-

bust transitions occur with a probability from the range $[0.0, 0.7917]$ and a mean of 0.4715, destructive transitions occur with a probability from the range $[0.0972, 0.9583]$ and a mean of 0.3210, and plastic transitions, when they exist, occur with a probability from the range $[0.0139, 0.6528]$ and a mean of 0.0481. The probability for a configuration to plastically change is found as the sum over all of its plastic transitions. For the configurations in *ON*, the probability of a plastic change occurs in the range $[0.0, 0.8194]$ with a mean of 0.1682. It is interesting to note that all configurations have a non-zero probability of both destruction and survival in this environment. The out-degree distribution of the network reflects the number of different plastic options available to an ontogenic trajectory at each viable configuration. This distribution is supported in the range $[0, 9]$ with a mean of 3.4935. Further, 30% of plastic transitions are bi-directional; a number that indicates the network has many more bi-directional edges than found in a random graph. Indeed, this hypothesis is supported by a p -value $\ll 0.001$ when comparing *ON* to an ensemble of 1000 random graphs with the same number of nodes and degree-distribution.

The graph theoretic structure of the viable configurations in *ON* reflects several interesting characteristics of ontogenies starting at configuration *SC* in environment \mathcal{E} . First, the number of viable configurations increases exponentially with minimum path-length from *SC*. Second, *ON* has several distinct clusters as highlighted by InfoMap network community detection [12] (Figure 4A). These graph-theoretic clusters reflect sets of configurations for which transitions are more likely to remain within the set than leave it. Third, there are several configurations which function as bottlenecks for the network in the sense that ontogenies must pass through those configurations to reach different areas of the network. These configurations are determined by high values of betweenness centrality [11].

Strongly connected components (SCCs) found in the current *ON* demonstrate irreversibility, branching, and attractors (Figure 4B). SCCs are sets of configuration in which all configuration are mutually reachable [11]. There are 32 SCCs in *ON*. The presence of multiple SCCs indicates irreversibility — if the system moves from one SCC to another, it cannot return. Branching is illustrated by diverging paths from the SCCs. If an individual exits an SCC along one branch, the alternatives can no longer be explored. Finally, those SCCs with no outgoing connections are attractors in the sense that if an ontogeny enters one of these sets, it is guaranteed to remain there until death.

The analysis of ontogenies is further enriched by considering their morphologies — their unique spatial arrangements of molecular concentrations. Recall that each configuration defines a point in the 3200-dimensional state space of *M* and *A* molecular concentrations. Due to their high dimensionality, these configurations are projected onto a 2-dimensional manifold using the IsoMap manifold identifi-

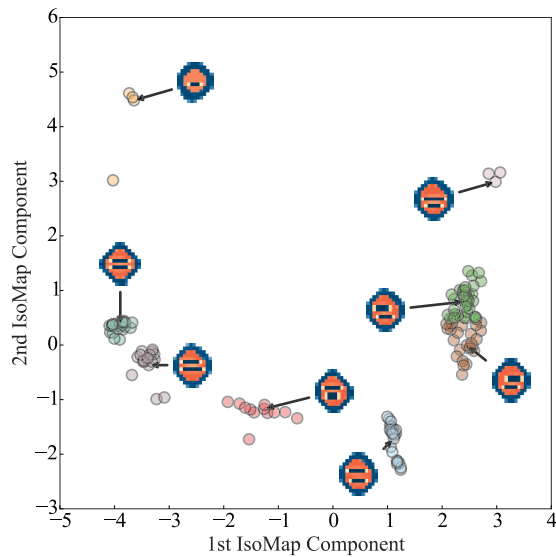


Figure 5: *ON*'s configurations, clustered according to morphological similarity. Each point is a single configuration's morphological state projected onto a two-dimensional space determined by two IsoMap components. Different colors represent clusters detected by K-means clustering. An exemplar configuration from each cluster illustrates the cluster's unique morphological features.

cation technique [13] including the whole set of other configurations as neighbors. The resulting projection, shown in Figure 5, had a reconstruction error of 1.8374. This projection is indicative of morphological clustering with many points tightly grouped and relatively large distances between the groups. Specific partitions of configurations can be identified using K-means clustering [9]. The resulting 8 clusters are shown using different colors in Figure 5. Comparison of the exemplar configurations from each cluster, identified by their central position relative to the cluster's mean, demonstrates how the clusters vary along several qualitative dimensions: the size of the configuration, the shape of the outer membrane, the thickness of the outer membrane, and the number and arrangement of internal membrane structures.

Combining the morphological similarity of viable configurations with the transition network structure of *ON* reveals that plastic transitions are much more likely to occur between morphologically-similar configurations. A Bayesian BEST test [8] between the distribution of all inter-configuration distances using the Euclidean metric and the distribution of configuration distances for those linked by a plastic transition shows that the means of the distributions are distinctly different, with an average difference of 3.25 in a 95% confidence interval of [3.16, 3.34]. There is also a strong correspondence between the morphological clusters and the InfoMap clusters previously identified in *ON* as reflected by a normalized mutual information [5] value of

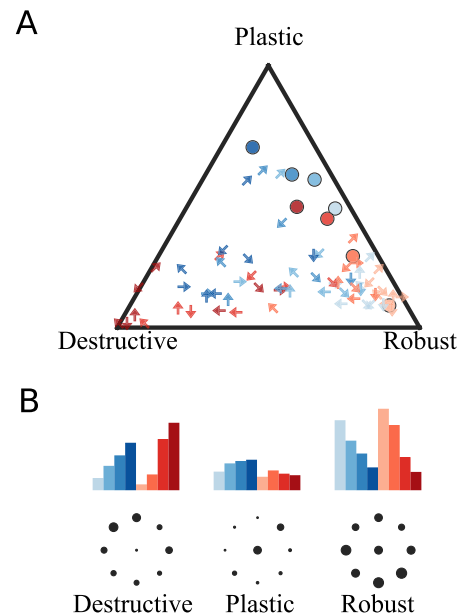


Figure 6: Environment \mathcal{E} 's 72 perturbations positioned according to their probabilities of inducing a robust, destructive or plastic transition when applied to a random configuration from *ON*. A) Perturbations are shown in barycentric coordinates with markers illustrating their location, type, and size. Arrows indicate the perturbation location on the outer membrane and circles indicate perturbations to the central position. Color indicates molecular type, either membrane (blue) or autocatalyst (red). The perturbation's magnitude is shown by the darkness of the marker, with darker markers indicating larger magnitudes. B) Histograms categorize the probability of perturbations inducing a destructive, robust, or plastic transition conditioned on (upper) the perturbations type and magnitude or (lower) location.

0.6746 between the two clusterings. Therefore, as an ontogeny unfolds and an individual falls into a graph-theoretic cluster, it also tends to maintain its morphological features by remaining within a corresponding morphological cluster.

In addition to characterizing attributes of the individual, the full ontogenetic network can also be used to characterize the influence of the environment. To proceed in the case of *SC* in \mathcal{E} , we return to the full ontogenetic network and classify each of the 72 perturbations by their probabilities of inducing a robust, destructive or plastic transition when applied to a random configuration from the set of viable configurations in *ON*. The resulting classification is visualized in Figure 6A according to barycentric coordinates for the three probabilities. Here, each point (arrow or circle) represents one of the 72 perturbations and the inverse distance between the point and each vertex reflects the associated probability of a transition in that equivalence class; a point directly on a vertex denotes 100% of transitions falling in that category.

Inspection of Figure 6A reveals that perturbations can vary widely in their consequences. Notably, all perturbations but one are destructive to at least one configuration, but none of the 72 perturbations are destructive to all configurations. There is a graduated tradeoff between perturbations' probabilities of inducing a robust transition versus inducing a destructive transition. A small subset of perturbations are associated with a large tendency to induce plastic transitions. These results can be further subdivided according to the location and magnitude of the applied perturbation as shown in Figure 6B. In the first row of the subfigure, three normalized histograms are shown which categorize perturbations based on outcome, molecular type (membrane in blue, autocatalyst in red), and magnitude (light to dark color). As one would expect, robust transitions are primarily associated with small perturbations while destructive transitions are associated with large perturbations. Plastic transitions occur more frequently for perturbations to membrane concentrations than to autocatalyst concentrations, regardless of magnitude. The second row of the subfigure illustrates three additional histograms categorizing perturbations based on outcome and location. These figures indicate that plastic transitions result more often from perturbations to the center and north-east locations while destructive transitions are slightly biased to perturbations on the north-west.

Quantifying viability and adaptivity

Viability is a consequence of well-matched configurations and environments. While some sequences of perturbations applied to an individual yield long ontogenies, the same individual exposed to different perturbations can result in shorter-lived ontogenies. The viability of a configuration is here defined as the expected lifespan over all of its possible ontogenies [2]. Two notions of adaptivity follow from this definition. Local adaptivity captures the change in viability resulting from a plastic transition: an adaptive transition increases a system's viability, a maladaptive transition reduces it. Global adaptivity is the general tendency for viability to increase with longer ontogenies.

In order to calculate viability, dynamics on an ontogenic network can be treated as a Markov chain. As a consequence of this, death becomes an absorbing state and most configurations are transients. Finding the average number of transitions from each transient state to an absorbing state is a well-studied problem [7], and gives our measure of viability. The lower bound on this measure is 1, which occurs when all perturbations bring the configuration to death within one step. The possibility of an immortal configuration would complicate this calculation by introducing infinite viability.

Applying these concepts to *ON* reveals a surprising abundance of adaptive transitions (Figure 7). The network's unsearched frontier is assumed to transition to death, giving a lower bound for the viability of all other configurations. A wide range of viabilities is found, from 1.0028 to 4.8382

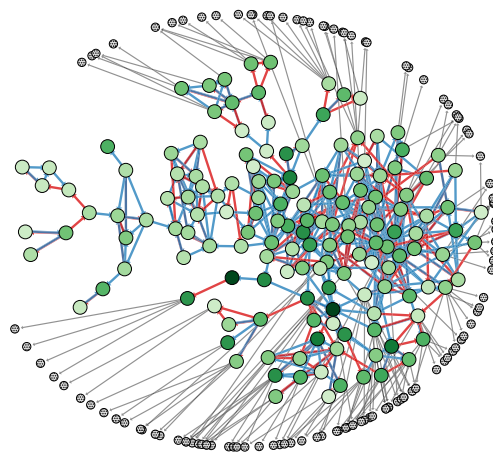


Figure 7: The network layout is the same as previous figures. Viability is shown by the darkness of the green nodes, locally adaptive transitions are blue, and locally maladaptive transitions are red.

with a mean of 2.1802, and 50% of the edges are locally adaptive. Interestingly, the most viable configuration in *ON* is not the most robust nor the one with the fewest destructive transitions. Its viability is a consequence of its embedding within the full ontogenic network.

Remarkably, ontogenies from *SC* also display global adaptivity. A correlation analysis found that a configuration's graph-theoretic path length from *SC* is positively correlated with its viability (r-value of 0.2882, p-value of 0.0003). This means that longer-lived ontogenies beginning at *SC* will generally experience an increase in expected lifespan. This global trend is configuration specific; each configuration in *ON* can have a different global adaptivity, and can even be globally maladaptive.

Mechanisms of adaptivity

This model provides an excellent opportunity to investigate the mechanisms underlying adaptivity. Previous formulations of adaptivity have assumed an explicit regulatory subsystem [3; 6]. This mechanism is designed to monitor the system's internal state relative to its boundary of viability and use this information to bring the system to more viable states. Models that implement this a priori assumption cover only a subset of possible mechanisms of adaptivity. In contrast, this paper's model demonstrates an emergent type of adaptivity. Analyzing the processes involved here can provide insights not previously possible.

As a first step towards understanding the mechanisms of emergent adaptivity, we examine a minimally adaptive scenario embedded within *ON*. An adaptive transition requires an environment of at least two perturbations, one which increases viability, the other which reduces it. Taken to its extreme, one perturbation would bring an initial configura-

tion to death, and the other perturbation would bring it to a second, immortal configuration. Multiple instances of this exact scenario are found embedded within ON when environment \mathcal{E} is restricted to only two perturbations.

The chosen example of a minimally adaptive scenario is shown in Figure 8A. The scenario begins with configuration α , which is subjected to the two perturbations. The perturbations are placed at different locations, but otherwise have the same magnitude and are both to the membrane field. On the top branch, α disintegrates, whereas on the bottom branch it undergoes a plastic transition to configuration β . β is then subjected to the same two perturbations, both of which result in robust transitions. In this minimal context, β can survive all perturbations, whereas α can survive only half of them. The transition from α to β is therefore adaptive.

One way to analyze this scenario is to utilize dynamical systems theory to characterize the system's phase space (Figure 8B). For visualization, the high-dimensional state space is projected onto the top two principal components. This makes trajectories appear to overlap, even though no overlap is possible in the full dynamics. Configurations α , β , and death are equilibrium points, each surrounded by a basin of attraction. The real basins of attraction are not visualizable, so faux basins of attraction are added to represent a hypothetical division of phase space. The two classes of perturbations (dashed red lines) instantaneously displace the system within the state space. Whereas perturbations to α move the system either to death's basin of attraction or to β 's basin of attraction, when applied to β they displace the system within the same basin of attraction. Given this analysis, adaptivity is explained by the congruence between the two configurations' basins of attractions and the available perturbations. The position of the equilibrium points, and the shape of their basins are such that the perturbed states fall outside of α 's basin, yet remain within β 's.

A more detailed investigation of mechanism needs to address the specific physico-chemical interactions that take place during this adaptive transition. A spatial analysis is here approached by taking sequential snapshots of transient configurations throughout the minimally adaptive scenario and identifying the critical differences in their morphologies (Figure 8C). First, we look at the adaptive transition from α to β (Figure 8C(1)) and the divergence from α that occurs throughout this transition (Figure 8C(2)). The sequence begins with α , at which there is no difference. Next, the perturbation displaces the membrane field, seen as a circular difference in the top right. Further down the sequence, the membrane concentration spreads around the boundary. While the north-east side of the configuration remains at increased concentrations, the rest of the boundary is slightly lower from its initial concentrations; this trait stabilizes at β . The most obvious difference between stable configuration β and α is a local increase in membrane concentration, which makes β rounder and thickens its boundary (arrow I).

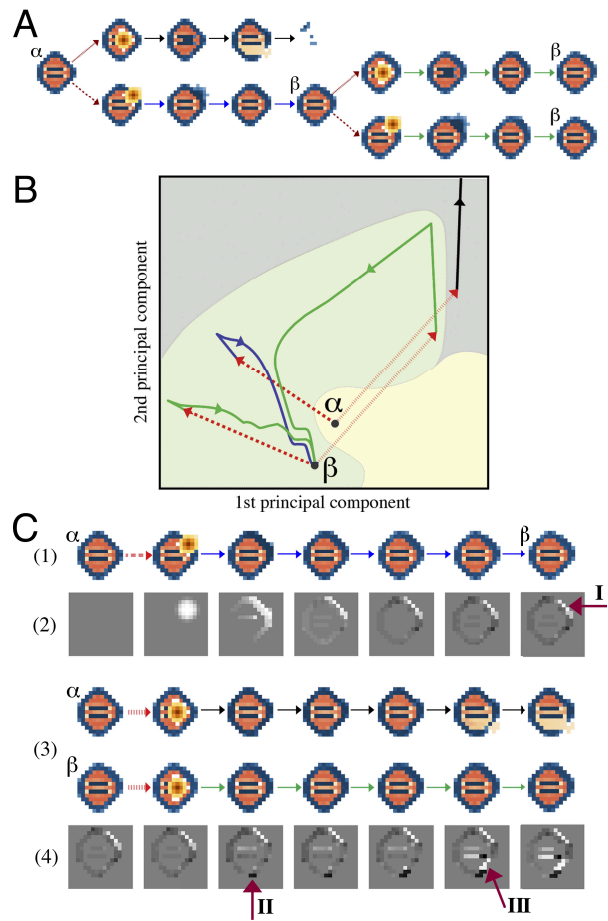


Figure 8: A minimally adaptive scenario and its analysis. A) Configuration α branches off into two transients following the application of two perturbations, one of which leads to disintegration, and the other to a plastic transition resulting in β . β is then perturbed by the same two perturbations and recovers, proving it has adapted. B) The same sequence of events shown in state space projected onto the top two principal components. Faux basins of attraction (yellow, green, gray regions) are added for explanatory purposes. Perturbations are indicated by the two classes of dashed red lines. Transients are shown as trajectories, with the destructive transition as a black trajectory, the adaptive plastic transition as a blue trajectory, and the robust transitions as green trajectories. C) The scenario is analyzed as sequences of spatio-temporal configurations. (1) The transition from α to β . (2) The difference from α 's membrane field for the corresponding sequence in (1); the figure is gray where membrane concentrations are the same as α , white where they are more than α , and black where they are less than α . (3) Both α and β 's responses to the second perturbation. (4) The difference between membrane concentrations for the two sequences in (3); where membrane concentrations are the same in these sequences, the figure is gray, where the transient following β has a higher membrane concentration, the figure is white, and where it has lower concentration, the figure is black.

Next, we examine how these morphological differences allow β to survive a perturbation that α does not survive (Figure 8C(3)). The difference between these two sequences shows where the relevant divergences begin (Figure 8C(4)). The sequence begins with the initial difference between α and β . When the perturbations are applied to both configurations, they do not appear in the difference plot because the perturbations are spatially aligned. Later, the behavior begins to diverge. The obvious difference between their initial structures (arrow I) is not where the fatal divergence begins. Instead, a region on the bottom of α (arrow II), which bulges out and to the right, is the important feature. This growth draws α 's membrane downward, reducing membrane concentration in the south-east boundary (arrow III). This opens up a tear in α 's membrane, from which autocatalyst pours out and ultimately brings about disintegration, whereas β 's morphology allows it to stay intact and restabilize.

In contrast with previous formulations of adaptivity, we see that no explicit regulatory mechanism is found during this emergent adaptive transition. Adaptivity is the result of distributed processes, and is better explained by their emergent spatio-temporal dynamics. The analysis demonstrates that local changes in chemical distributions, such as thickening membranes, have consequences for subsequent behavior. In dynamical systems terms, adaptivity is determined by the shape of configurations' basins of attraction, and how interactions with the environment move a system through the phase space. A transition is adaptive if it brings the individual to a configuration with a more accommodating basin.

Discussion

This paper marks the first analysis of ontogeny in a spatial chemical model that supports emergent individuality. The ontogenic network is a unique consequence of the individual's morphology paired with a particular environment. A combination of statistical and graph-theoretic methods revealed a rich structure, which includes clusters and bottlenecks that constrain ontogenic change. The reachable morphologies were found to cluster according to morphological similarity, and we showed that as an individual falls into a graph-theoretic cluster it tends to maintain its morphological features. Two notions of adaptivity followed from the definition of viability as average expected lifespan; local adaptivity looks at the change in viability resulting from plastic transitions, and global adaptivity looks at longer-term increases in viability. There was an abundance of local adaptivity within the ontogenies, and surprisingly, the model also displayed global adaptivity. Finally, the mechanisms of a minimally adaptive scenario were analyzed, demonstrating how adaptivity can be explained by distributed process rather than explicit regulatory mechanisms.

The combination of this model and analytical techniques provides a foundation for studying the emergence of viability, ontogeny, and adaptivity in more biologically real-

istic systems. One natural extension along these lines reconceptualizes viable configurations as members of dynamically richer limit sets. Another recognizes that environments also include sequential perturbations that occur on similar or faster timescales compared to an individual's intrinsic dynamics; these environments would keep the system from stabilizing at a limit set and require a new, continuous conceptualization of ontogenic change. Further, biological individuals and environments are structurally coupled [10], suggesting that an individual's behavior could induce correlations in its environment which affect future interactions. All of these factors need to be considered in a generalization of adaptivity to real-world biological individuals.

Acknowledgements

This work was supported by NSF grant IIC-1216739, and Lilly Endowment, Inc., through its support for the Indiana University Pervasive Technology Institute, and by the Indiana METACyt Initiative. The software is freely available at https://github.com/eagmon/co-construction_base

References

- [1] Agmon, E., Gates, A. J., Churavy, V., and Beer, R. D. (2014). Quantifying robustness in a spatial model of metabolism-boundary co-construction. *ALIFE 14: The Fourteenth Conference on the Synthesis and Simulation of Living Systems*, 14:3–5.
- [2] Agmon, E., Gates, A. J., Churavy, V., and Beer, R. D. (in press). Exploring the space of viable configurations in a model of metabolism-boundary co-construction. *Artificial Life*.
- [3] Ashby, W. R. (1960). *Design for a Brain*. Springer.
- [4] Beer, R. D. (2014). The cognitive domain of a glider in the game of life. *Artificial life*, 20(2):183–206.
- [5] Danon, L., Daz-Guilera, A., Duch, J., and Arenas, A. (2005). Comparing community structure identification. *Journal of Statistical Mechanics: Theory and Experiment*, 2005(09):P09008.
- [6] Di Paolo, E. A. (2005). Autopoiesis, adaptivity, teleology, agency. *Phenomenol Cogn Sci*, 4(4):429–452.
- [7] Grinstead, C. M. and Snell, J. L. (1998). *Introduction to Probability*. American Mathematical Soc.
- [8] Kruschke, J. K. (2013). Bayesian estimation supersedes the t test. *Journal of Experimental Psychology: General*, 142(2):573.
- [9] Lloyd, S. (1982). Least squares quantization in pcm. *IEEE Transactions on Information Theory*, 28(2):129–137.
- [10] Maturana, H. R. and Varela, F. J. (1980). *Autopoiesis and cognition: The realization of the living*. Number 42. Springer.
- [11] Newman, M. E. (2003). The structure and function of complex networks. *SIAM review*, 45(2):167–256.
- [12] Rosvall, M. and Bergstrom, C. T. (2008). Maps of random walks on complex networks reveal community structure. *PNAS*, 105(4):1118–1123.
- [13] Tenenbaum, J. B., De Silva, V., and Langford, J. C. (2000). A global geometric framework for nonlinear dimensionality reduction. *Science*, 290(5500):2319–2323.